



e-ISSN: 2319-8753 | p-ISSN: 2320-6710

IJRSET

International Journal of Innovative Research in
SCIENCE | ENGINEERING | TECHNOLOGY



INTERNATIONAL JOURNAL OF INNOVATIVE RESEARCH

IN SCIENCE | ENGINEERING | TECHNOLOGY

Volume 9, Issue 10, October 2020

ISSN INTERNATIONAL
STANDARD
SERIAL
NUMBER
INDIA

Impact Factor: 7.512

9940 572 462

6381 907 438

ijirset@gmail.com

www.ijirset.com

Simple Quantum Mechanical Modelling of Single Electron Fault in QCA

Amar Prakash Sinha

Dept. of Electronics and Communication Engineering, BIT Sindri, Dhanbad, India

ABSTRACT: A simple model of single electron fault (SEF) of Quantum-dot cellular automata (QCA) is proposed in this work. The wavefunctions and energy levels of the SEF in QCA cell and its effects on subsequent QCA cells are presented. Imaginary time propagation technique and Hartree-Fock technique for obtaining the solutions of Schrodinger's equation for simulation of the faulted QCA cells has been adopted. It is observed that the polarity of the subsequent QCA cell is inverted when compared to the normal case due to presence of SEF in a QCA cell. A systematic methodology is presented to encounter this problem. The basic target of this paper is to present simple quantum mechanical modelling of QCA

KEYWORDS: Quantum-dot cellular Automata (QCA), Single Electron Fault (SEF), quantum dots, coupling of QDs, coulombic interaction, fault tolerance.

I. INTRODUCTION

Silicon CMOS technology has been governing IC industry for about five decades. Electronic IC manufacturing and its impact on every aspect of life has seen tremendous growth. Trends of growth in IC technology has been following Moore's law [1] so far. Device feature size has been shrinking down to few nanometers. This incredible growth in CMOS technology has brought it to a stage where researchers are looking for alternative of CMOS or CMOS with alternate structure [2]. Reasons include quantum mechanical behaviour of electron at low dimension, power dissipation, leakage currents, parasitic capacitances etc. In spite of using high K material at gate, the amplification factor is reducing tremendously with size. A paradigm shift with quantum devices is seemingly inevitable. QCA has emerged as a promising alternative to current CMOS VLSI. QCA is introduced to create nano-scale devices with high compaction density capable of performing computation at high switching speed. It was first proposed by Toffoli [3] but the solid state structure was proposed by Lent et. al [4]. Initially, the structure was proposed with five QDs, but eventually it was established that very stable structure can be made using four QDs [5]. Rigorous research is going on towards the implementation of complex logic structure in QCA [6,7,8].

A QCA is composed of array of interactive cells, each cell having four QDs arranged at four corners of the square shaped cell. The centre to centre distance between two cells is appreciably more than the distance of two QDs of same cell to avoid tunnelling of electron between cells. Every cell is assumed to have two electrons located diagonally due to coulombic interaction. The major interaction between the cells is coulombic force. Figure 1 shows the structure of the QCA cells. Position of electrons in subsequent cell are dependent on the position of electrons in preceding cell. This is how the polarization is propagated through the cells. Majority gate and inverter are the basic logical operations based on QCA [4].

Nanoscale devices, like QCA, are susceptible to high error rate. The faults in QCA structure has become a significant area of research [9,10,8]. The effect of temperature has been addressed and modelled since the introduction of QCA and still being discussed [4,10]. Some of the faults and defects associated with QCA are stray charge defect, shifted device defect, missing cell defects, single electron fault, three electron fault, misshapen fault etc [11]. Since, the position of electron influences the signal transition and propagation, it is important to investigate all the physical faults related to electron and/or dot in QCA cells [12,13].

The problem of fault and fault tolerance in QCA structure is addressed by solving Hamiltonian, and most popular model is tight-binding Hubbard-type Hamiltonian with Coulomb repulsion which is usually solved using Hartree-fock method [14,15,16]. We found that a simpler method, with added post simulation work, can be exploited. Presented model uses a very fast method proposed by R. Kossloff [17] which has been adapted for coupled QD systems [18,19,20]. We have used this imaginary time technique to obtain the energy eigenvalues and wavefunction for addressing a simple quantum mechanical modeling of SEF in QCA. The results obtained is compared with the results obtained with Hartree-Fock technique. Mahdavi et.al. also presented simple model for SEF, but that method used only electrostatic energy estimation [12,13,21]. However quantum mechanical modeling is expected to give better results at nanoscale. In this work we have described the QCA cell and its operation in section II. In section III, we have discussed the formulation of problem. Computational method has been described in section IV. We have presented the results for

variation of positions of single electron in QCA and its effect on subsequent QCA in section V. Conclusions and an approach to tackle the effect of SEF are presented at last.

II. DESCRIPTION OF QCA

Figure 1 gives schematic of the ideal QCA cell structures in ground state, which have four identical QDs represented as open circles, forming corners of a square. We assume two electrons, represented by solid dots, in each cell occupying the diagonal positions. The polarization is defined as given in figures 1(a) and (b), anticlockwise position to be -1 polarization ($P = -1$) and clockwise position to be +1 polarization ($P = +1$) respectively.

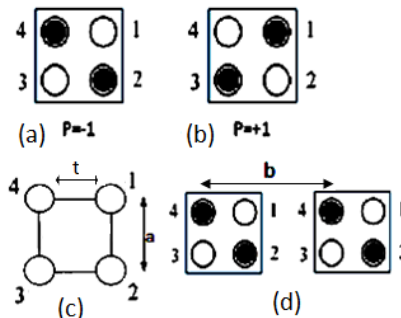


Figure 1: Ideal QCA cells, with (a) -1 polarization (b) +1 polarization, (c) dimensions of the cell (d) intercellular distance.

In a cell the electrons are allowed to jump between the individual QDs using quantum mechanical tunnelling. In an isolated cell the electron will occupy the diagonal dots at ground state due to the coulombic force possessing either of polarization. This gives a bistable latch like behaviour with only two stable states. The nearby cells have sufficient barrier in form of intercellular distance, to completely suppress the tunnelling to occur between adjacent cells. Coupling between two adjacent cells is governed by the coulombic interaction and clocking action. Figure 2 shows the coupling between the adjacent cells which compels cell 2 to have the same polarization as cell 1.

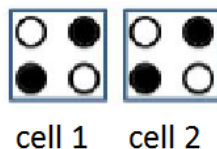


Figure 2: Cell 2 has the same polarization as cell 1 due to coulombic interaction.

The physical interaction between cells may be used to realize elementary Boolean functions. The basic logic gates using QCA structure are given in figure 3.

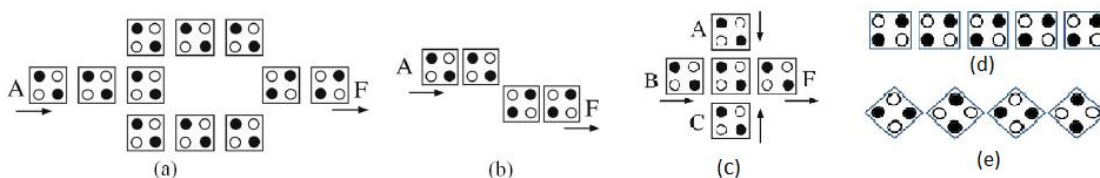


Figure 3: (a) Redundant inverter gate, (b) Inverter gate, (c) Majority logic gate, (d) Binary wire and (e) Inverter chain.

Majority logic function given in figure 3(c) is the most important logic gate, with which we can implement OR gate when one input is permanently fixed to logic 1, and AND gate can be implemented fixing one input to logic 0. Clocking is very important aspect of QCA, which not only provides a mean for synchronizing information flow along the circuit, but also controls the direction of information flow in a QCA circuit. The QCA clock also provides the power required for the logic operations. Actually, the clock is used to control the tunnelling barrier height of QD in a QCA cell. Clocking scheme can be divided into four regions as given in figure 4(a). When clock gets low, the electron gets trapped in QD and cannot tunnel to other QD. This is the hold phase. When the clock signal is high, all QD's barrier gets lower and electrons are free to move. This may be called to be null polarization state or relax phase.

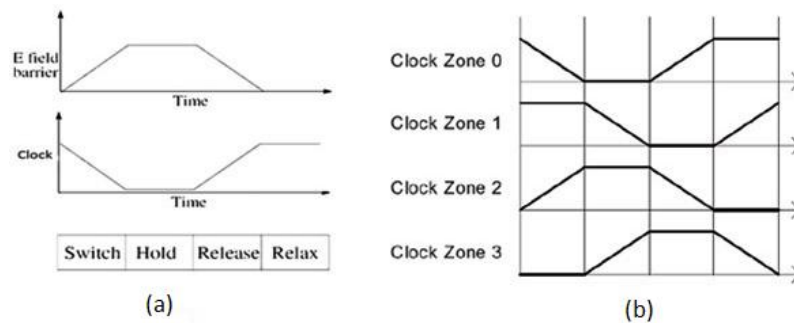


Figure 4: (a) Clocking scheme, clock regions and corresponding barrier potential, (b) QCA clock Zone

Figure 4(b) shows QCA clock, each cell in a particular clocking zone is connected to one of the four available phases of the QCA clock. Each cell in the particular clock zone is latched unlatched, and synchronized with the changing clock signal [22].

III. Formulation of problem

We have taken QCA as described in figure 1 in last section. Figure 1(c) gives the dimensions of one cell. In our case the centre to centre distance between two neighbouring QDs, $a=9\text{nm}$, interdot distance t is 4nm , and the dot diameter is 5nm . The distance between the centres of two adjacent cells is 20nm (let us call this distance to be 'b' for using it in equations). For example, considering two neighbouring cells, the distance between dot 4 in the left cell and dot1 in the right cell is 29nm . We have taken InAs dots on GaAs substrate in our studies. The band offset between InAs and GaAs at conduction band is considered to be 570meV . All dimensions are taken in AU for simulation. The confinement potential of QDs is considered to have Gaussian shape. Also we have assumed that, each cell is assigned to an individual clock zone and there are no neighbour cells in the same clock zone.

Here we are addressing Single Electron Fault (SEF), in which we assume that a single QCA cell in between the binary wire or inverter chain has only one electron as shown in figure 5. Figures 5(a) and 5(b) show the effect of SEF in binary wire and 5(c) and 5(d) shows the effect on inverter chain.

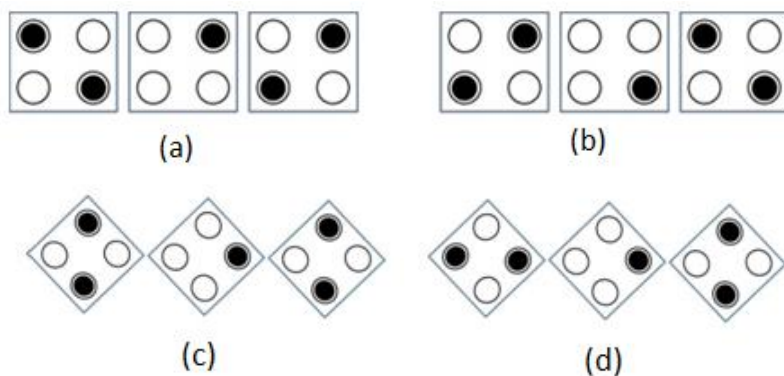


Figure 5: Single Electron Fault (a), (b) in binary wire, and (c), (d) in inverter chain.

We can observe that the effect of single electron logically inverts the expected result. It adversely affects the operations of QCA. To verify this result we must model the QCA cells using quantum mechanical modelling. In this paper we have proposed that the QCA structure can be modelled and simulated with a simple model and simpler method of solving Hamiltonian. This model has been used to address the single electron fault.

IV. METHOD OF SOLVING THE PROBLEM

We have used a very fast method proposed by R. Kossloff [17] for solving Hamiltonian, which has been adopted by many authors as well as in our earlier paper with slight modifications [20]. This method is based on imaginary time propagation technique.



The method can be described in three steps.

- a. An assumed form of wavefunction is specified over a two dimensional grid.
- b. Calculation of the Hamiltonian operation on this assumed wavefunction.

$$\psi, \psi = H\psi, \psi \tag{1}$$

where ψ is the assumed wavefunction and Hamiltonian H is given by Eq. (2). The potential energy operator term is obtained by straight forward multiplication of $V_{x,y}$ and $\psi_{x,y}$ over the grid. The kinetic energy operator term can be computed more efficiently in the inverted space domain by taking FFT followed by multiplication with $(2\pi k)^2$ and subsequent inverse FFT operation.

- c. In this major step, wave function is propagated over imaginary time axis.

$$\psi = e^{-Ht} \psi_0 \tag{2}$$

Where ψ_0 is wavefunction at $t=0$, an arbitrary function can be expanded as a linear combinations of eigenfunctions of the Hamiltonian Eq. (3) dictates that each eigenfunction relaxes to zero exponentially at the rate determined by the eigenvalue. This implies that the ground state relaxation is the slowest, and hence will be the only state to persist. The propagation can be easily carried out by expanding e^{-Ht} in terms of Chebychev polynomial:

$$e^{-Ht} = \sum_{n=0}^N a_n T_n(HR) \tag{3}$$

where $a_n = 2I_n(R)$, for $n > 0$ and $a_0 = I_0(R)$, I_n is the n^{th} modified Bessel's function of the first kind and R is the range of eigenvalues represented on the grid multiplied by τ (the time of propagation):

$$R = \sqrt{V_{\text{max}} - V_{\text{min}} + 2\delta x^2 + 1\delta y^2} \tag{4}$$

T_n is the real Chebychev polynomial which is calculated by the recursion:

$$T_n(X) = 2XT_{n-1}(X) - T_{n-2}(X) \tag{5}$$

and $T_0(X) = 1$, $T_1(X) = X$ and $X = HR$

For higher eigenvalues we use projection operator. The first excited state is obtained by removing the ground state from the Hilbert space. This makes the first excited state the ground state of the new space. If $P_0 = |0\rangle\langle 0|$ is the projection operator of the groundstate, then the ground state for the operator:

$$H_1 = H - P_0 H P_0 \tag{6}$$

is the first excited state. This procedure is repeated, to obtain the next excited state by removing the lower states.

To optimize the result we first take a guess of wavefunction on a coarse grid and carry out propagation operation. The wavefunctions thus obtained is used as new assumption and is propagated on a finer grid. This can be done in recursion to optimize the result. Another optimization can be done with taking small propagating time initially and then repeat the process to avoid loss of normalization.

Now the wavefunction as obtained by the above procedure can provide the probability of electron found at any QD. Here we are assuming that when the clock is high (in relaxed phase for a given QCA cell) and the tunnelling height is lowered the electron has tendency to get to the QD with highest probability density. Following assumptions are made to simplify the model.

- I. We are concerned about the probability density and we have not modelled the presence of two or more electron in the cell. However special treatment is done to compensate this anomaly.
- II. We have not considered the spin state of electron.

The Hamiltonian of the specified cell includes the confinement potential of QDs and coulombic energy of the preceding cell. Hence the Hamiltonian of the second cell when first cell has polarization $p = -1$, is given by

$$-\frac{\hbar^2}{2m} \nabla^2 \psi + V_{x,y} \psi = E \psi \tag{7}$$

where potential $V_{x,y}$, is given by

$$V_{x,y} = V_0 \exp(-a^2 x^2 - y^2 + q_2 a^2 x - b + a^2 x^2 + y^2 + q_2 a^2 x - b - a^2 x^2 + y^2 + a^2 x^2 + y^2) \quad 8$$

Here a and b are dimensions as described in figures 1(c) and 1(d), ϵ_{sc} is the relative permittivity of the semiconductor QD (This has to be added in recursion for coordinates x and y). Using the technique described in this section the wavefunction and energy eigenvalue are deduced. From the wavefunction, we calculate the probability density of the electron at different QDs.

The wavefunction obtained by imaginary time propagation technique for single electron has been used as guess function in our work to save time of convergence.

The results are described in next section.

For simulations all the dimensions are taken in atomic unit (AU).

V. RESULTS AND DISCUSSION

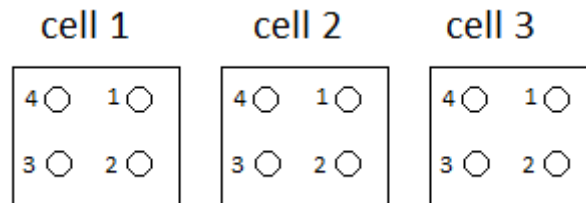


Figure 7: Three interacting QCA cells.

Following are the results of calculation of probability densities of electrons at different sites of a cell as given in the figure 6.

Case 1. First of all cell 2 is simulated assuming no effect of the neighbours. The probability densities of different sites are found to be equal, and it is found to be 0.250 for all sites.

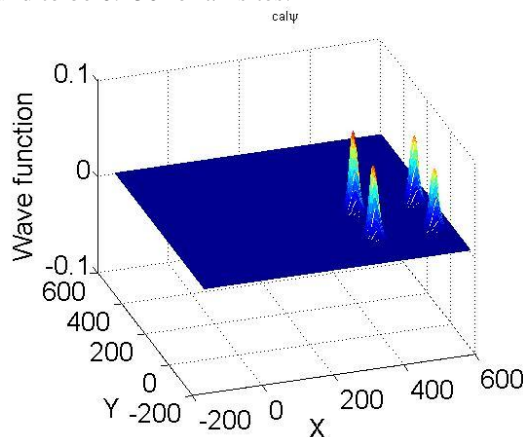


Figure 8: Wavefunction of a QCA cell without the effect of neighbouring cells.

The wave function is shown in figure 7. This indicates that if there is no interaction between two cells, the polarity of the cell can be either of +1 or -1 with same probability and electrons are filled in either of the diagonal positions.

Case 2. Cell 2 is assumed to have the SEF, with cell one having the polarity $p = -1$ and the second cell is simulated. We got the probability densities at sites 1, 2, 3 and 4 respectively in cell 2 as 0.428, 0.390, 0.069 and 0.116. The wavefunction and confinement potentials are shown in figure 8

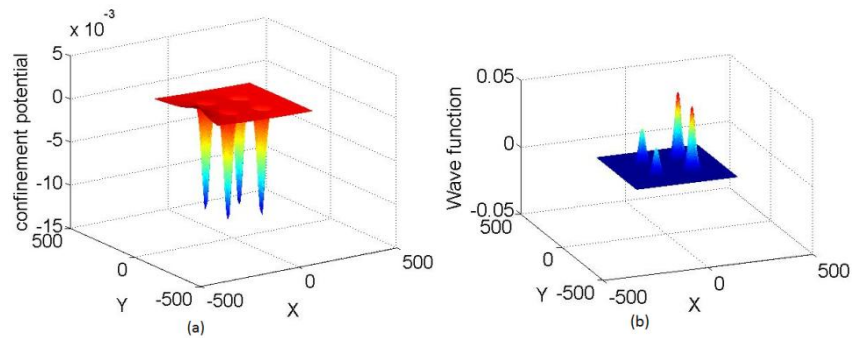


Figure 9: (a) Confinement potential and (b) wavefunction for cell no. 2 when cell 1 has -1 polarity.

This establishes that when cell 2 has SEF the single electron has highest probability to be at site 1, if cell 1 has polarity $p = -1$.

Now starting with cell 1 to have the polarity of -1, and cell 2 has the single electron at site 1 then in cell 3 the probability densities, at sites 1 to 4, respectively are 0.342, 0.394, 0.177 and 0.091. Confinement potential and wavefunction are shown in figure 9,

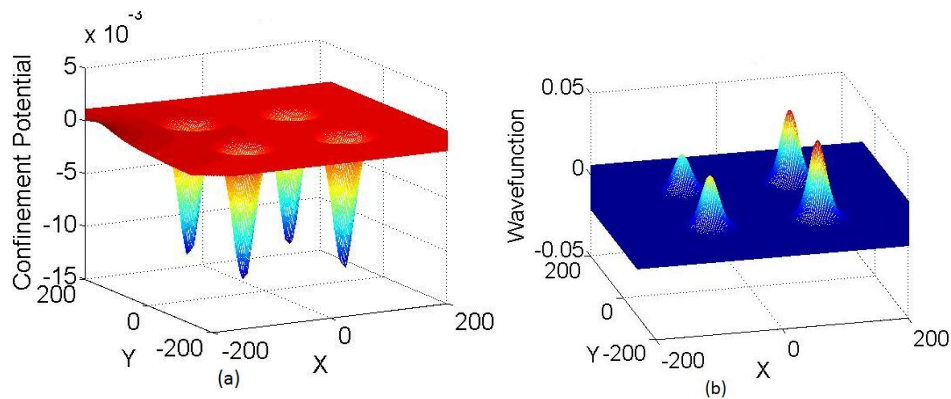


Figure 10: Confinement potential and wavefunction for cell no. 3 when cell 2 has SEF and electron is at site 1.

This simulation establishes half part of the complete picture as it provides the greatest probability at one of the site for single electron. We are dealing with two electrons and interaction between them has to be accounted and yet simpler modelling has to be done. This kind of simulation can only give the probability of one electron nicely as the single particle Hamiltonian has been considered. As mentioned in introduction further simulations will have to be carried out to find the position of both electrons in the 3rd cell. Simulations have been done for the second electron in 3rd cell with one electron fixed at one of the sites. Obviously four simulations have been done and then inferences have been made. Sub cases are explained as follows.

Case 2.1. With fixed position of one electron in cell 3:

With -1 polarity in cell 1, one electron at site 1 in cell 2 and one electron at site 1 in cell 3 the corresponding probability densities at sites 2, 3 and 4 respectively are 0.413, 0.532 and 0.095, respectively, and total energy is -0.005594. Confinement potential and wavefunction is shown in figure 10.

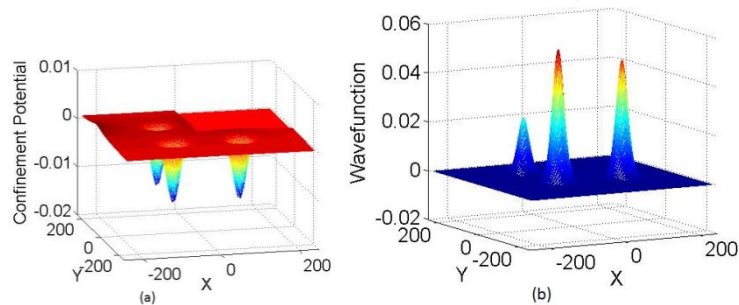


Figure 11: Confinement potential and wavefunction of cell 3 when one electron of cell 2 is at site 1 and one electron in cell 3 is fixed at site 1.

This establishes that site 3 is most likely to be occupied by the other electron in cell 3 in this condition. Electrons at sites 1 and 3 provide a stable diagonal combination.

Case 2.2. To find the only stable condition let us take, one electron at site 1 in cell 2 and one electron at site 2 in cell 3, the corresponding probability densities at sites 1, 3 and 4 are 0.494, 0.255 and 0.377, respectively, and the energy is -0.005541. Confinement potential and wavefunction is shown in figure 11.

Thus site 1 has the largest probability, but if site 1 is filled it will compel the other electron to go to site 3 as simulated in case 2.1. This has established that the most stable position of electrons in 3rd cell will be at diagonal sites 1 and 3.

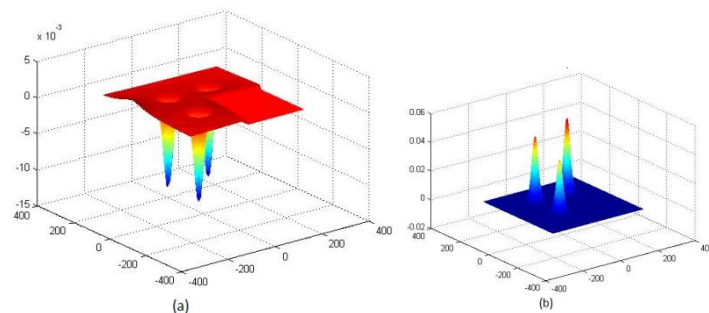


Figure 12: Confinement potential and wavefunction of cell 3 when one electron of cell 2 is at site 1 and one electron in cell 3 is fixed at site 2.

Case 2.3. Continuing likewise we have fixed the position of one electron at site 3 in cell 3, the corresponding probability densities at sites 1, 2 and 4 are 0.682, 0.273 and 0.063, respectively, and the energy is -0.005668. Wavefunction is shown in figure 12.

This simulation provides a stable diagonal combination similar to case 2.1 and strengthen the probability of electrons to occupy site 1 and 3 to make the polarity of cell 3 as +1.

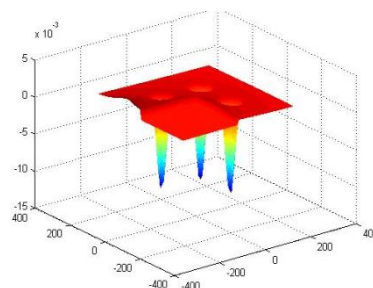


Figure 13: Wavefunction of cell 3 when one electron of cell 2 is at site 1 and one electron in cell 3 is fixed at site 3.

Case 2.4. Finally with one electron fixed at site 4 in cell 3, the corresponding probability densities at sites 1, 2 and 3 are 0.212, 0.703 and 0.110, respectively, and the energy is -0.005680. Wavefunction is shown in figure 13. This seems to be a stable situation as the electron has maximum probability to be at the diagonal sites 4 and 2, but actually once one electron goes to site 2 this will follow the case 2.2 and again the electron from site 4 will jump to site 1, and eventually the electron from site 2 will jump to site 3 presenting +1 polarity.

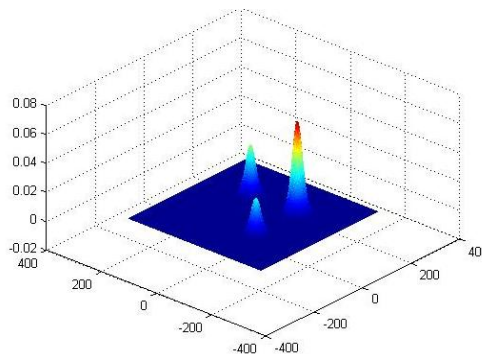


Figure 14: wavefunction of cell 3 when one electron of cell 2 is at site 1 and one electron in cell 3 is fixed at site 4.

Combining all the cases (2.1 to 2.4) it has been inferred that in this case the polarity of 3rd cell will be +1 in this case.

Case 3. Similarly for polarity to be +1 at cell 1, we get the probability densities at sites 1, 2, 3 and 4 respectively in cell 2 as 0.390, 0.428, 0.116 and 0.069. Confinement potential and wavefunction is shown in figure 13.

Thus it is established that when cell 2 has SEF, the single electron is most likely to be at site 2 if cell 1 has polarity of +1.

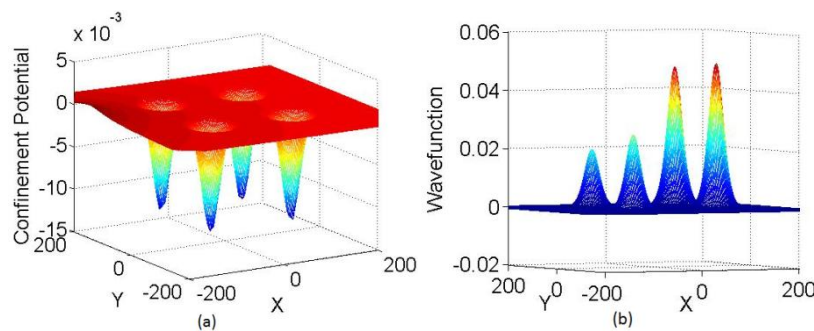


Figure 15: Confinement potential and wavefunction for cell no. 2 when cell 1 has +1 polarity.

Similarly when cell 1 has the polarity of +1 and assuming that cell 2 has single electron at site 2, then in cell 3 the probability densities respectively are 0.394, 0.342, 0.091 and 0.177.

With procedure similar to case 2 and as briefed in table 1 it can be established that if cell 1 has polarity of -1 and cell 2 has SEF then cell 3 has polarity of +1 and if cell 1 has polarity of +1 and cell 2 has SEF then cell 3 has the polarity of -1.

Table 1: Compilation of the results

Cases	Condition	Considered Cell	Probabilities through the different sites				Inferences (with highest probability)
			Site 1	Site 2	Site 3	Site 4	
Case 1	Assuming no effect of the neighbours (cell 1)	---	0.250	0.250	0.250	0.250	Same probabilities for both polarities (+1 and -1).
Case 2	Assuming -1 polarity at cell 1 and cell 2 having SEF	Cell 2	0.428	0.390	0.069	0.116	Site 1 is filled with the single electron
Case 2.1	Same as case 2 and one electron of cell 3 fixed at site 1	Cell 3	---	0.413	0.532	0.095	Second electron will be at site 3, creating stable combination.
Case 2.2	Same as case 2 and one electron of cell 3 fixed at site 2	Cell 3	0.494	---	0.255	0.377	Second electron will be at site 1 making unstable combination.
Case 2.3	Same as case 2 and one electron of cell 3 fixed at site 3	Cell 3	0.682	0.273	---	0.063	Second electron will be at site 1 making stable condition
Case	Same as case 2 and one	Cell 3	0.212	0.703	0.110	---	Second electron may be at site 2 viz. stable

2.4	electron of cell 3 fixed at site 4						but whence one electron is at site 2, case 2.2 is followed viz. unstable
Case 2: Started with -1 polarity at cell 1 and SEF at cell 2 results cell 3 with +1 polarity							
Case 3	Assuming -1 polarity at cell 1 and cell 2 having SEF	Cell 2	0.390	0.428	0.116	0.069	Site 2 is filled with the single electron
Case 3.1	Same as case 2 and one electron of cell 3 fixed at site 1	Cell 3	—	0.494	0.377	0.255	Second electron will be at site 2, making unstable combination.
Case 3.2	Same as case 2 and one electron of cell 3 fixed at site 2	Cell 3	0.413	—	0.095	0.532	Second electron will be at site 4 creating stable combination.
Case 3.3	Same as case 2 and one electron of cell 3 fixed at site 3	Cell 3	0.703	0.213	—	0.110	Second electron may be at site 1 viz. stable but whence one electron is at site 1, case 3.1 is followed viz. unstable
Case 3.4	Same as case 2 and one electron of cell 3 fixed at site 4	Cell 3	0.273	0.682	0.063	—	Second electron will be at site 2, creating stable combination.
Case 3: Started with +1 polarity at cell 1 and SEF at cell 2 results cell 3 with -1 polarity							

With these observations it can be concluded that SEF changes the polarity of the proceeding cells in QCA wire.

VI. CONCLUSIONS

We have proposed a simple model for simulating QCA. Single electron fault is dealt in detail, which shows that it has an alarming effect. Other faults like effect of temperature, stray charge defect, shifted device defect, missing cell defects, single electron fault, three electron fault, misshapen fault can be modelled and simulated through this method. As a remedy to this problem, whenever we deal with binary wire we can have two more redundant wire and use majority gate at last before the next logic operation. This will decrease the probability of error in great extent.

REFERENCES

- [1]G. E. Moore, "Cramming more Components onto Integrated Circuits," Electronics, vol. 38, no. 8, p. 114, Apr. 1965.
- [2]S. Gupta, V. Moroz, L. Smith, Q. Lu, and K. C. Saraswat, "7-nm FinFET CMOS Design Enabled by Stress Engineering Using Si, Ge, and Sn," IEEE Transaction on Electronic Devices, vol. 61, no. 5, pp. 1222-1230, May 2014.
- [3]N. Margolus and T. Toffoli, "Cellular Automata Machines," MIT Press, cambridge: Complex Systems, vol. 1, pp. 967-993, 1987.
- [4]C. S. Lent, P. D. Tougaw, and P. Wolfgang, "Bistable Saturation in Coupled Quantum Dots for Quantum Cellular Automata," Appl. Phys. Lett., vol. 62, no. 7, pp. 714-716, Feb. 1993.
- [5]P. D. Tougaw and C. S. Lent, "Dynamic Behavior of Quantum Cellular Automata," J. Appl. Phys., vol. 80, no. 8, pp. 4722-4736, Oct. 1996.
- [6]V. Pudi and K. Sridharan, "Efficient Design of a Hybrid Adder in Quantum-Dot," IEEE Transaction on Very Large Scale Integration (VLSI) System, vol. 19, no. 9, pp. 1535-48, Sep. 2011.
- [7]K. Sridharan and V. K. Pudi, Design of Arithmetic Circuits in Quantum Dot Cellular Automata Nanotechnology, 1st ed. Switzerland: Springer International Publishing, 2015.
- [8]B. Sen, et al., "Towards the Design of Hybrid QCA Tiles Targeting High Fault Tolerance," Journal of Computational Electronics, vol. 15, pp. 429-445, Jun. 2016.
- [9]M. Momenzadeh, M. B. Tahoori, J. Huang, and F. Lombardi, "Quantum Cellular Automata: New Defects and Faults for New Devices," in Proceedings of the 18th International Parallel and Distributed Processing Symposium, 2004, pp. 207-214.
- [10]G. A. Anduwan, et al., "Fault-tolerance and Thermal Characteristics of Quantum-dot Cellular Automata Devices," Journal of Applied Physics, vol. 107, no. 11, pp. 1134061-10, Jun. 2010.
- [11]M. Crocker, X. S. Hu, and M. Niemier, "Defects and Faults in QCA-Based PLAs," ACM Journal on Emerging Technologies in Computing Systems, vol. 5, no. 2, pp. 8:1-8:27, Jul. 2009.
- [12]M. Mahdavi, S. Mirzakuchaki, M. N. Moghaddasi, and M. A. Amiri, "Single Electron Fault Modelling in Quantum Binary Wire," IET Micro Nano Letters, vol. 6, no. 2, pp. 75-77, Feb. 2011.



- [13]M. Mahdavi, S. Mirzakuchaki, M. N. Moghaddasi, and M. A. Amiri, "Single Electron Fault Modeling in Basic Quantum Devices," Japanese Journal of Applied Physics, vol. 50, p. 094401, Sep. 2011.
- [14]D. Pfannkuche, V. Gudmundsson, and P. A. Maksym, "Comparison of a Hartree, a Hartree-Fock, and an Exact Treatment of Quantum-dot Helium," Physical Rev. B, vol. 47, no. 4, pp. 2244-2250, Jan. 1993.
- [15]M. Governale, M. Macucci, G. Iannaccone, and C. Ungarelli, "Modeling and Manufacturability Assessment of Bistable Quantum-dot Cells," Journal of Applied Physics, vol. 85, no. 5, pp. 2962-2971, Mar. 1999.
- [16]C. S. Lent, B. Isaksen, and M. Lieberman, "Molecular Quantum-Dot Cellular Automata," Journal of American Chemical Society, vol. 125, no. 4, pp. 1056-1063, Apr. 2003.
- [17]R. Kosloff, "A Direct Relaxation Method for Calculating Eigenfunctions and Eigen Value of the Schrodinger Equation on a Grid," Chemical Physics Letters, vol. 127, no. 3, pp. 224-230, Jun. 1986.
- [18]S. Badnarek, "Effective Interaction for Charge Carriers Confined in Quasi-one-dimensional Nanostructures," Physical Review B, vol. 68, no. 4, pp. 0453281-9, Jul. 2003.
- [19]S. Badnarek, "Time-evolution Simulation of a Controlled-NOT Gate with Two Coupled Asymmetric Quantum Dots," Physical Review A, vol. 71, no. 6, pp. 0623271-8, Jun. 2005.
- [20]A. P. Sinha, J. Kumar, and V. Kumar, "Effect of Separation and Electric Field on Single Electron States of Lateral Quantum Dots," Journal of Nanoelectronics and Optoelectronics, vol. 10, no. 5, pp. 616-622, Oct. 2015.
- [21]M. Mahdavi, M. A. Amiri, S. Mirzakuchaki, and M. N. Moghaddasi, "Single Electron Fault Modeling in QCA Inverter Gate," Canadian Journal on Electrical & Electronics Engineering, vol. 1, no. 1, pp. 20-24, Feb. 2010.
- [22]M. A. Amiri, M. Mahdavi, and S. Mirzakuchaki, "QCA Implementation of a MUX-Based FPGA CLB," in International Conference On Nanoscience and Nanotechnology, Australia, 2008, pp. 141-144.



INNO SPACE
SJIF Scientific Journal Impact Factor

**Impact Factor:
7.512**

ISSN INTERNATIONAL
STANDARD
SERIAL
NUMBER
INDIA



INTERNATIONAL JOURNAL OF INNOVATIVE RESEARCH

IN SCIENCE | ENGINEERING | TECHNOLOGY

 9940 572 462  6381 907 438  ijirset@gmail.com



www.ijirset.com

Scan to save the contact details